# Impact of random fabrication errors on backward-wave small-signal gain in traveling wave tubes with finite space charge electron beams

Sean Sengele,[1,a),b)] Marc L. Barsanti,[2] Thomas A. Hargreaves,[2] Carter M. Armstrong,[2] John H. Booske,[3] and Y. Y. Lau[4]
[1]*Sensors and Electromagnetic Applications Laboratory, Georgia Tech Research Institute, Smyrna, Georgia 30080, USA*
[2]*L-3 Communications – Electron Devices Division, San Carlos, California 94070, USA*
[3]*Department of Electrical and Computer Engineering, University of Wisconsin – Madison, Madison, Wisconsin 53706, USA*
[4]*Department of Nuclear Engineering and Radiological Sciences, University of Michigan, Ann Arbor, Michigan 48109, USA*

(Received 6 November 2012; accepted 5 February 2013; published online 21 February 2013)

A one-dimensional small-signal theory for the backward-wave mode in a traveling-wave tube (TWT) is developed, which includes the effects of random fabrication errors. This is of interest since the backward-wave mode is the spatial harmonic typically responsible for instability in a TWT. The described model examines how gain and instantaneous 1-dB bandwidth of the backward-wave mode is affected by random fabrication errors, which are modeled as random perturbations of the phase velocity, interaction impedance, and loss along the TWT's length. Random variation of the phase velocity is found to have the largest effect on both the backward-wave gain and the bandwidth while having only a minor effect on fundamental, forward-wave mode behavior. © *2013 American Institute of Physics*. [http://dx.doi.org/10.1063/1.4792666]

## I. INTRODUCTION

Vacuum electronic amplifiers offer significant potential for high output power with relatively high efficiency, bandwidth, and overall performance in the millimeter-wave (mm-wave) and terahertz (THz) regimes for radar, communications, electronic warfare, and scientific applications.[1,2] With nominal feature sizes proportional to their operational wavelengths (approximately 1 to 0.1 mm), the dimensional accuracy and precision required to fabricate these devices become increasingly stringent. A single fabrication error on the order of even a few microns can represent a significant deformation to a structure of this size.

For any spatially periodic structure, such as a helix slow-wave structure (SWS) in a traveling-wave tube (TWT), the total electromagnetic (EM) wave propagating along its length can be described as a sum of spatial harmonic modes that all have the same frequency but different propagation vectors.[3] In the case of the helix SWS, the "fundamental" or "forward" mode is the lowest order mode and represents a wave with a phase and group velocity in the +z direction. The "backward-wave" mode is a separate spatial harmonic mode and represents a wave with an effective phase velocity in the +z direction but a group velocity in −z. Thus, the backward-wave mode can still exchange energy with the traveling electron beam in a TWT (also traveling in the +z-direction) even though its energy flow is in the opposite direction. The coupling of energy to the backward-wave mode is the primary cause of unwanted oscillations in a TWT that is designed to be an amplifier.

Pierce theory[4–6] has been previously adapted to analyze the effects of random fabrication errors on the fundamental, forward-wave mode.[7,8] Similarly, Chernin *et al.*[9] have explored the effect of random fabrication errors on TWT gain and output phase including the effect of multiple internal RF reflections from arbitrarily positioned discontinuities (i.e., fabrication errors). They observed that both the gain and the insertion phase of the TWT were more significantly impacted than were originally reported by Pengvanich *et al.*[7] They also observed that these reflections could cause significant gain ripple versus frequency.

Building on the work by Pengvanich *et al.*, we reformulated the Pierce-type model to be applicable for the backward-wave mode in a TWT with random fabrication errors and a finite space-charge electron beam. This allowed us to examine the impact of fabrication errors (encoded as random variations in the Pierce parameters along the length of the simulated TWT) on *backward-wave* gain and bandwidth.

## II. THEORY

The model is derived in a similar manner as was done for the fundamental forward-wave mode[7,8] but is reformulated for the backward-wave mode and includes the effect of space charge on the electron beam. There are two necessary equations to formulate this model, namely, the "electronic" and "circuit" equations. The "electronic" equation, which describes the motion of the electrons in the TWT, is given as

$$\left[\left(\frac{\partial}{\partial z}+j\beta_e\right)^2+\beta_q^2\right]s=a, \tag{1}$$

where $\beta_e \equiv \omega/u_0$ is the wavenumber associated with the electron beam disturbance, $\omega$ is the operational frequency of

[a)]Sean.Sengele@gtri.gatech.edu.
[b)]Previously with the Department of Electrical and Computer Engineering, University of Wisconsin – Madison, Madison, Wisconsin 53706, USA.

 

the TWT, and $u_0$ is the dc velocity of the electron beam. The parameter $\beta_q \equiv \omega_q/u_0$ is the reduced space-charge wavenumber where $\omega_q \equiv R_{sc}\omega_p$, $R_{sc}$ is the "plasma frequency reduction" factor[5,6,10] in which the beam's plasma frequency is given by $\omega_p^2 \equiv e\rho/(m\epsilon_0)$, $\rho$ is the volume charge density of the beam, $e$ and $m$ are the charge and rest mass of an electron, respectively, and $\epsilon_o$ is the permittivity of free space. MKS units were used for all variables.

The $R_{sc}$ is introduced to acknowledge that the space charge force term is not only linearly related to the charge density in the electron bunches of the beam but also limited by the fact that the electron beam is finite in diameter and in close proximity to image charges in nearby conducting surfaces. The value of $R_{sc}$ does not impact the conclusions that can be drawn from the model however. Instead of attempting to use accurate predictions for the value of $R_{sc}$, we opt to vary the value of the normalized Pierce parameter for space charge, $4QC$, which, by definition, includes $R_{sc}$. The determination of $R_{sc}$ is beyond the scope of this work.

The variable, $s = \tilde{i}_1$, is a variable substitution for the ac beam current used to make the nomenclature match previous work.[7,8] The parameter $a \equiv -je\lambda_0\beta_e^2\tilde{E}'_z/(m\omega)$ is the normalized electric field acting on the electron beam element where $\lambda_0$ is the linear charge density of the beam and $\tilde{E}'_z$ represents the complex magnitude of the axially directed electric field of the RF wave propagating along the SWS. Equation (1) is the same as the electronic equation used for the fundamental forward-wave mode[8] since they both describe the same electron beam.

The "circuit" equation describes the behavior of the RF wave on the SWS induced by the beam's modulated current. Since the goal is to model a backward-wave mode in a TWT, this equation is derived from a transmission-line model in which the phase and group velocities travel in opposite directions.[4,6,11] Doing so gives

$$\left(\frac{\partial}{\partial z} + j\beta_p - \beta_p C d\right) a = j(\beta_e C)^3 s, \tag{2}$$

where $\beta_p \equiv \omega/v_p$ is the "cold" circuit wavenumber of the RF field as it propagates on the SWS without the beam present and $v_p$ is the cold circuit phase velocity. The parameter, $C^3 \equiv I_0 K/(4V_0)$, is the dimensionless Pierce gain parameter where $I_0$ is the dc electron beam current and $V_0$ is the beam voltage corrected for space charge depression. The Pierce interaction impedance of the circuit is given by $K \equiv |E_z|^2/(2\beta_p^2 P_z)$ where $E_z$ is the axial component of electric field of the RF wave on the circuit and $P_z$ is the total RF power flowing along the SWS as given by Poynting's theorem. The parameter, $d$, is the normalized cold circuit loss rate which is greater than zero.

Comparing the circuit equations of the backward-wave mode given here with the fundamental forward-wave mode,[8] it is observed that the only difference between the two are negative signs on the $d$ and $s$ terms. The sign of the loss parameter, $d$, ensures that RF loss rate occurs in the same direction as the group velocity of each respective mode while the sign of $s$ is determined from the underlying circuit model from which each mode's circuit equation is derived. This corresponds well with conventional Pierce theory (without fabrication errors) where previous authors[4,5] have shown that the fundamental forward-wave and backward-wave circuit equations differ by similar negative signs.

Invoking Ramo's theorem,[12] we assume that the modulated electron current in the electron beam induces equivalent currents in the SWS. This allows Eqs. (1) and (2) to be combined to form a single 3rd-order differential equation. This is simplified by first defining a normalization variable, $f$, such that

$$s = e^{-j\beta_e z} f(x) = e^{-jx} f(x), \tag{3}$$

where $x \equiv \beta_e z$ is the phase length along the SWS. Combining Eqs. (1) through (3) gives

$$\frac{d^3 f(x)}{dx^3} + jC(b+jd)\frac{d^2 f(x)}{dx^2} + C^2(4QC)\frac{df(x)}{dx} + jC^3[(4QC)(b+jd) - 1]f(x) = 0, \tag{4}$$

where $b \equiv (\beta_p - \beta_e)/(\beta_e C) = (u_0 - v_p)/(v_p C)$ is the Pierce velocity parameter, and $4QC \equiv [\beta_q/(\beta_e C)]^2 = R_{sc}^2\omega_p^2/(\omega^2 C^2)$ is the Pierce space-charge parameter. For a given TWT design, the value of 4QC for the backward wave mode is likely different than for the forward wave mode. However, estimates using conventional formulas[13] indicate that the values of 4QC will likely not be different enough to significantly impact our conclusions.

It is worthwhile to point out that these equations do not take into account either RF wave reflections from the discontinuities or coupling between the forward and the backward waves. Although previous authors have demonstrated that these issues can significantly impact TWT performance,[9,14] we have left them out of our model in order to limit its complexity. The addition of these physics is left for future work.

Next, the initial conditions for Eq. (4) are defined at the input of the device, $z = 0$, which corresponds to the phase length, $x = 0$. From Eq. (3), $f(x)$ is proportional to the ac beam current, $s$, which is assumed to be zero at $x = 0$. The parameter $f'(x) = df(x)/dx$, which is proportional to the ac velocity of the electron beam element (assuming a time-harmonic solution), is also assumed to be zero at $x = 0$. Finally, using Eqs. (1) and (3), it can be shown that $f''(x) + C^2(4QC)f(x)$ is proportional to the normalized axial RF electric field, $a$, where $f''(x) = d^2 f(x)/dx^2$. Since the magnitude of the electric field at the input of the TWT is an arbitrary value and since $f(0) = 0$, we set $f''(0) = 1$. In summary, at the TWT input, $x = 0$, the initial conditions of the differential equation are given as

$$\begin{aligned} f(0) &= 0, \\ f'(0) &= 0, \\ f''(0) &= 1. \end{aligned} \tag{5}$$

Finally, the power gain of the backward-wave mode is defined as

$$Gain_{BW} = \frac{\left|f''(0) + C^2(4QC)f(0)\right|^2}{\left|f''(x) + C^2(4QC)f(x)\right|^2} = \left|\frac{1}{f''(x) + C^2(4QC)f(x)}\right|^2. \quad (6)$$

For constant and uniform $b$, $C$, $d$, and $4QC$, Eq. (4) can be reduced to the determinantal equation given by the conventional Pierce model[4] if a spatial harmonic solution is assumed. That is, if $a$ and $s$ are assumed to vary as $e^{j\beta z}$, Eq. (4) can be reduced to

$$\xi^2 - \frac{1}{(\xi - b - jd)} - 4QC = 0, \quad (7)$$

where the RF wavenumber in the presence of the electron beam is assumed to differ from the electron beam's wavenumber by a small amount, $\xi$ (i.e., $\beta = \beta_e + \beta_e C\xi$ where $|C\xi| \ll 1$). Equation (7) is identical to Pierce's determinantal equation although Pierce used $j\delta$ instead of $\xi$.

## III. RESULTS

Equation (4) was solved subject to the boundary conditions defined in Eq. (5) while the Pierce parameters $b$, $C$, and $d$ were simultaneously allowed to independently vary randomly along the phase length, $x$, of the simulated TWT. We did not explore the direct effect of independent random variations of the space charge parameter, $4QC$, however. This was neglected since random fabrication errors are expected to induce only a small, neglectable variation of the space charge parameter.

Similar to previous publications,[7,8] the Pierce parameters were assumed to be piece-wise linear functions along the length of the TWT. For this series of simulations, we defined the randomly varied Pierce parameters at $x = 1, 2, 3,\ldots$ which, according to Eq. (3), correspond to fabrication errors with a correlation length of $1/\beta_e$.

The value of the Pierce parameters at each of these "nodes" along the TWT's length was assumed to be an independent Gaussian random variable with a specified mean and standard deviation. An example of the piece-wise linear function is shown in Fig. 1. We denote the mean value as $\mu$ and the standard deviation as $\sigma$. For example, we specify the velocity parameter as $b = b_0 + b_1$ where $b_0 = \mu_b$ is the mean value and $b_1$ is a Gaussian random number defined by the standard deviation, $\sigma_b$. Only one Pierce parameter was allowed to vary during a given simulation. It is acknowledged that random fabrication errors would likely affect all the Pierce parameters simultaneously but, by simulating the effects independently, it is easier to identify which type of error has the greatest potential impact on TWT performance.[7]

For each specific standard deviation, the calculation of Eq. (4) was repeated 1000 times. The Pierce parameters were independently randomized along the length of the TWT for each trial giving a different piece-wise linear function for each. The results did not significantly differ when 500 or 2000 trials were simulated.

For each trial, the gain was calculated at each phase length, $x$, according to Eq. (6). Over the ensemble of trials, the mean and standard deviation of the gain at each $x$ phase length were calculated. The *maximum* mean gain, and its corresponding standard deviation and length were then determined and stored. An example of the calculated mean normalized power (inversely related to the gain) is given in Fig. 2(a) in which the corresponding maximum gain occurs near $x = 60$.

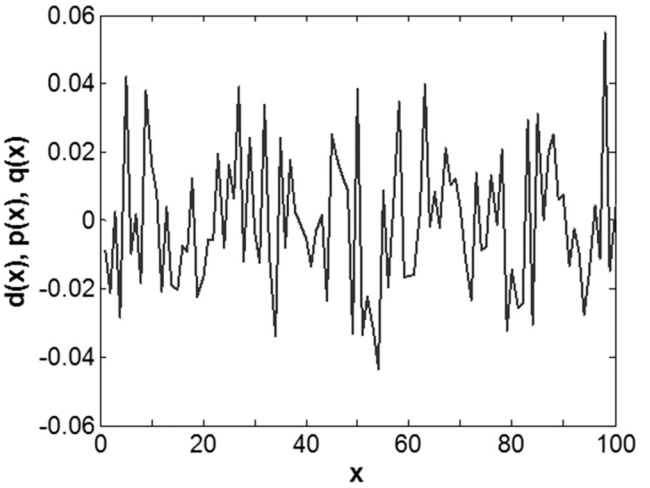


FIG. 1. Example of piece-wise linear function used to simulate the randomly varied Pierce parameters. In this case, the mean was set to zero and the standard deviation was set to 0.02.

The calculation of gain was repeated over a band of $b_0$ values. Assuming a constant electron beam voltage, varying $b_0$ equates to varying the phase velocity (and thereby synchronism) of the RF wave. Since $b_0$ is directly related to the beam/RF synchronism, we calculated the full-width 1-dB

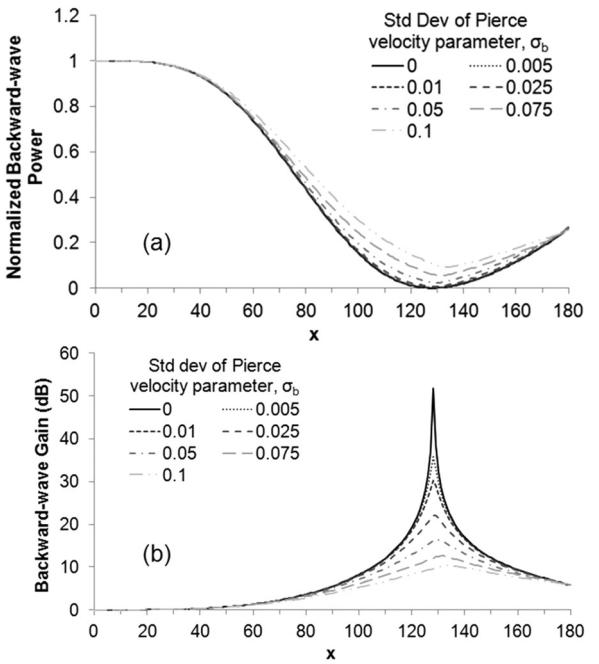


FIG. 2. (a) Example of mean RF power, $|f''(x) + C^2(4QC)f(x)|^2$, versus the axial phase length, x, for various Pierce velocity parameter errors and (b) corresponding backward-wave maximum mean gain as calculated by Eq. (6). In this example, $C = 0.035$, $d = 0$, $b_0 = 2$, and the number of trials was 1000.

bandwidth of the maximum mean gain with respect to $b$ and used it to estimate the effect of errors on instantaneous spectral bandwidth of the backward-wave mode. Additionally, simulating multiple $b_0$ values allowed us to track the change in the location of the maximum gain (with respect to $b_0$) when fabrication errors were introduced.

In order to maintain consistent results as $b_0$ was varied, the piece-wise linear function representing the Pierce parameters remained constant for all $b_0$ values in a given trial. In other words, although the Pierce parameters were randomly varied along $x$ for a given trial, they remained constant as $b_0$ was varied. In doing this, the effects of fabrication errors are assumed to be frequency independent for each series of simulations.

It is important to note from Fig. 2(a) that, for the error-free case ($\sigma_b = 0$), the normalized backward-wave *power* approaches zero near $x = 130$ (i.e., the output end of the TWT) which corresponds to the backward-wave mode *gain*, shown in 2(b), approaching infinity. This is expected since, in the ideal error-free case, a TWT has an absolute instability assuming it is made sufficiently long. The infinite gain could not be captured numerically, however, since an absolute numerical tolerance of $10^{-5}$ was applied to the differential equation solver used to solve Eq. (4). Thus, the maximum calculated gain is limited to approximately 50 dB.

### A. Random variation of the RF phase velocity

Random fabrication errors in the construction of a TWT can result in random variation of the RF phase velocity along its length. Similar to previous work,[7,8] we described these errors using $q(x) \equiv (v_q(x) - v_{q0})/v_{q0}$, where $v_{q0}$ is the unperturbed RF phase velocity of the backward-wave mode (i.e., the phase velocity of the backward-wave on the SWS without fabrication errors present). The relationship between $\sigma_q$ and the standard deviation of the Pierce velocity parameter, $\sigma_b$ is given by $\sigma_b = (\sigma_q/C)(1 + Cb_0)$.

An example of the calculated error-free backward-wave gain versus the axial length, $x$, and mean Pierce velocity parameter, $b_0$, is given in Fig. 3. In this example, $x = 0$–$180$, $C = 0.019$, $4QC = 1.85$, $d = 0$, and $\sigma_q = 0$ (i.e., there are no velocity perturbations along the length of the TWT).

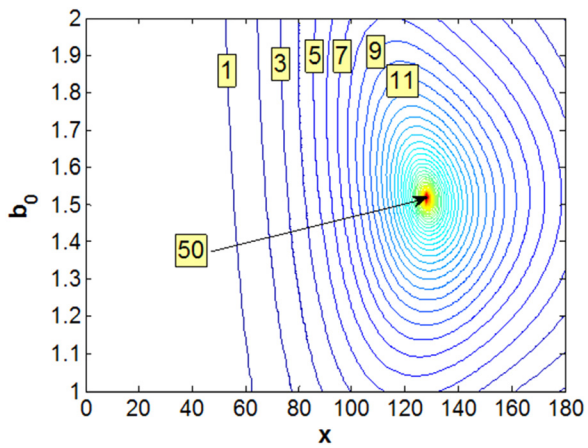


FIG. 3. Calculated error-free, backward-wave mode gain versus axial distance, $x$, and Pierce velocity parameter, $b_0$. In this example, we used $C = 0.019$, $4QC = 1.85$, and $d = 0$. No fabrication errors were simulated ($\sigma_q = \sigma_p = \sigma_d = 0$). The values specified in the boxes on the contour lines represent the backward-wave mode gain on that line in dB.

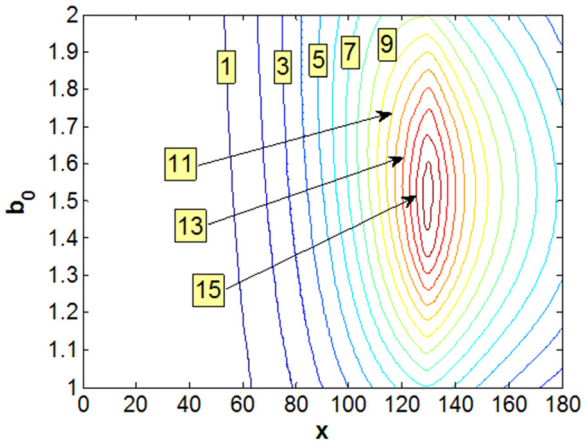


FIG. 4. Calculated backward-wave mode gain averaged over 1000 trials (each trial having a different random distribution of phase velocity errors) versus axial distance, $x$, and Pierce velocity parameter, $b_0$. In this example, we used $C = 0.019$, $4QC = 1.85$, $d = 0$, and a phase velocity error, $\sigma_q = 5\%$. The values specified in the boxes on the contour lines represent the backward-wave mode gain on that line in dB.

Figure 3 shows that there is a very specific $x$ and $b_0$ location at which the maximum gain occurs when no errors are present. This $x$-value corresponds to the so-called, "start oscillation-length" for the TWT while the $b$-value is related to the oscillation frequency via the dispersion diagram. Although the backward wave gain is expected to approach infinity at the exact oscillation length, this simulation is limited to numerically finite values, thus, the maximum gain is approximately 50 dB near $b_0 = 1.5$ and $x = 130$.

Phase velocity errors were then introduced ($\sigma_q = 0.05$) and the gain recalculated. The calculation was repeated 1000 times, each time with a different random piece-wise linear function for the phase velocity along $x$. The results are given in Fig. 4. Each $x$, $b_0$ point represents the mean gain of the 1000 trials. Thus, the figure represents 3 600 000 individual simulations (1000 trials at each 180 $x$-positions

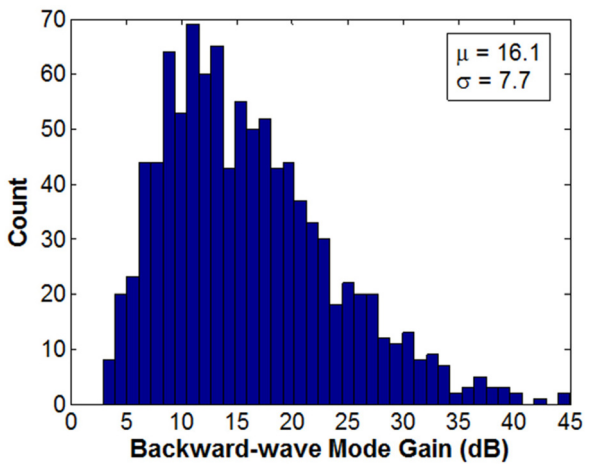


FIG. 5. Distribution of maximum calculated backward-wave mode gain at $x = 129$ for $C = 0.019$, $4QC = 1.85$, and $d = 0$. A 5% phase velocity error, $\sigma_q$, was simulated. The calculated Gaussian mean, $\mu$, and standard deviation, $\sigma$, of the distribution are given in the upper right corner.

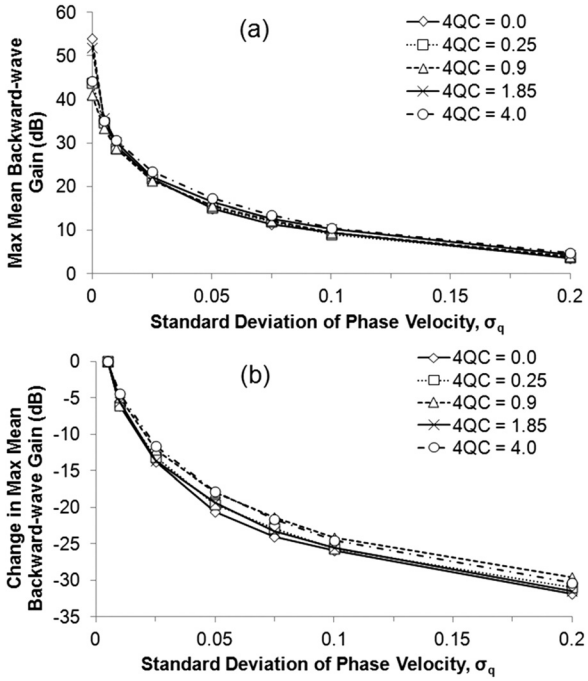


FIG. 6. Variation of maximum mean backward-wave mode gain for $C = 0.019$ and $d = 0$ at different $4QC$ values as a function of the magnitude of random SWS phase velocity errors. The unnormalized results presented in (a) are normalized to the $\sigma_q = 0.005$ case for each $4QC$ value in (b). The gain is expected to approach infinity at $\sigma_q = 0$ but is numerically limited to a finite number.

and 20 $b_0$-positions). The gain is significantly suppressed from the error-free case and occurs over a wider band of $b_0$ values (i.e., over a wider band of frequencies). The resultant backward-wave mode gain has a maximum of approximately 16.5 dB near $b_0 = 1.5$ and $x = 130$.

Further examination of the distribution of the calculated backward-wave gain over the 1000 simulated trials was completed by plotting the distribution of the *maximum* gain (with respect to $b_0$) at a fixed axial length, in this case, $x = 129$. The distribution is shown in Fig. 5. The calculated mean and standard deviation are 16.0 dB and 7.6 dB, respectively. Although this distribution is not precisely Gaussian, Gaussian statistics were used to approximately describe the mean and standard deviation of the gain distributions since they are widely understood and allowed for easy comparison with

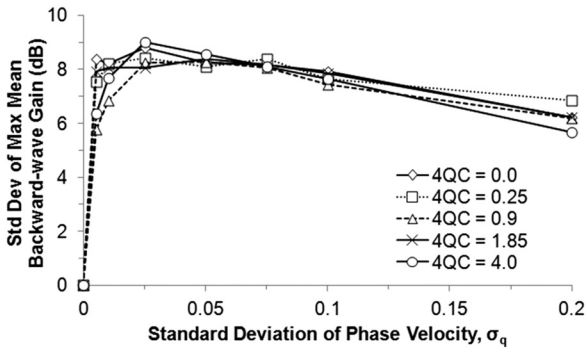


FIG. 7. Standard deviation of maximum mean backward-wave mode gain for $C = 0.019$ and $d = 0$ at different $4QC$ values as a function of the magnitude of random SWS phase velocity errors.

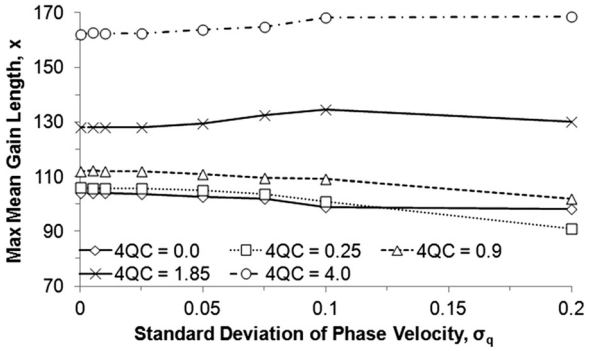


FIG. 8. Variation of length at which the maximum mean gain occurs with $C = 0.019$ and $d = 0$ at different $4QC$ values as a function of the magnitude of random SWS phase velocity errors.

previous publications.[7,8] A better fit statistical distribution may be interesting for subsequent studies but is beyond the scope of this analysis.

Figures 6(a) and 6(b) show the absolute and relative variation of the maximum mean backward-wave mode gain as a function of the magnitude of phase velocity error at different $4QC$ values. These simulations were completed using $C = 0.019$ and $d = 0$. Figure 7 shows the corresponding standard deviation. Figure 8 shows the corresponding axial TWT lengths at which the maximum mean backward-wave mode gain occurs (the $\sigma_q = 0$ points equal the start oscillation length for an ideal, error-free SWS).

Figure 9 gives the calculated full-width instantaneous 1-dB bandwidth of the maximum mean gain in terms of $b$ for the same series of simulations. Since the bandwidth is calculated from the maximum mean gain, it is expected that the error-free case has zero bandwidth regardless of the value of $4QC$. This is because the error-free maximum mean gain includes the absolute instability which has an idealized zero bandwidth in addition to infinite gain.

### B. Random variation of the interaction impedance

Random variations of the Pierce gain parameter, $C$, were also examined. Since the cube of $C$ is linearly proportional to the interaction impedance of the circuit, this is equivalent to testing the effect of random variations of the interaction impedance. Again, similar to previous analysis,[7,8] we describe the random variation as $C^3(x) = C_0^3[1 + p(x)]$ where $C_0$ is the

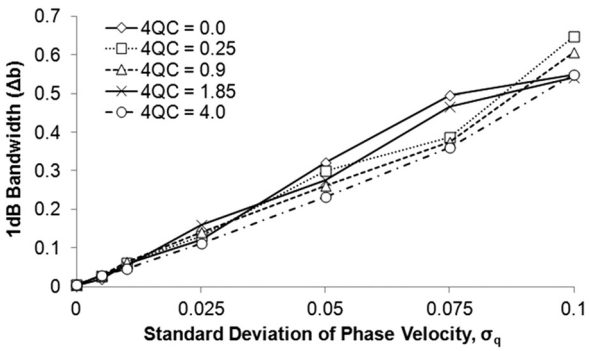


FIG. 9. Variation of 1-dB bandwidth of maximum mean gain in terms of $b$ for $C = 0.019$ and $d = 0$ at different $4QC$ values as a function of the magnitude of random SWS phase velocity errors.

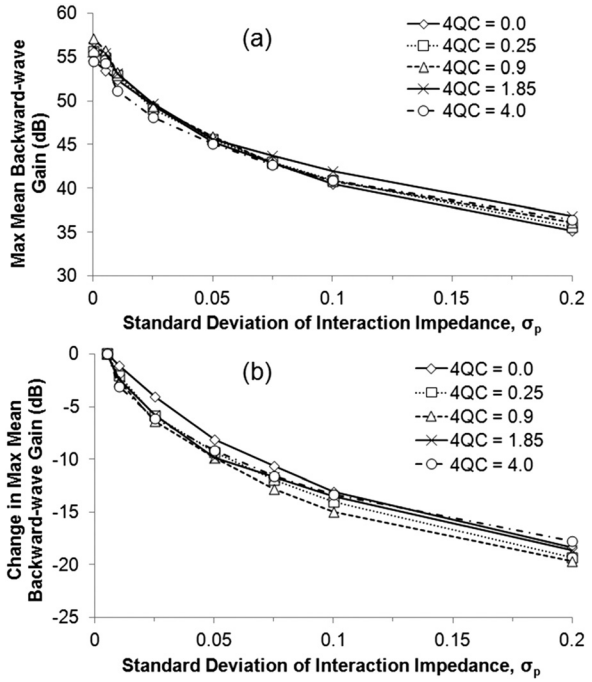


FIG. 10. Variation of maximum mean backward-wave mode gain for $C_0 = 0.019$ and $d = 0$ at different $4QC$ values as a function of the magnitude of random interaction impedance errors. The unnormalized results presented in (a) are normalized to the $\sigma_p = 0.005$ case for each $4QC$ value in (b).

unperturbed Pierce gain parameter (i.e., the value of $C$ that corresponds to the SWS without fabrication errors present) and $p(x)$ is a normally distributed, spatially dependent random number having a standard deviation of $\sigma_p$. The correlation between $\sigma_p$ and $\sigma_C$ is given as $\sigma_C = C_0\sigma_p/3$.

During these simulations, the value of the space charge parameter, $4QC$, was self-consistently calculated as $C$ was varied since $4QC$ depends intrinsically on $C$. We assumed that the electron beam parameters (i.e., voltage, current, and charge density) remained constant for each simulation; therefore, the change in $4QC$ is given as $4QC(x) = [C_0^2/C^2(x)]4QC_0$ where $4QC_0$ is the unperturbed space charge parameter.

Figures 10(a) and 10(b) show the absolute and relative variation of the maximum mean backward-wave mode gain as a function of the magnitude of Pierce gain parameter error at different $4QC$ values. These simulations were completed

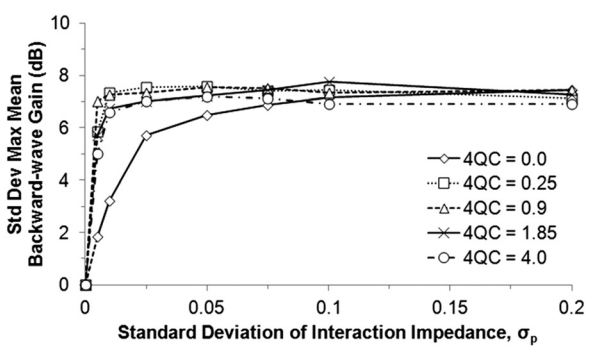


FIG. 11. Standard deviation of maximum mean backward-wave mode gain for $C_0 = 0.019$ and $d = 0$ at different $4QC$ values as a function of the magnitude of random interaction impedance errors.

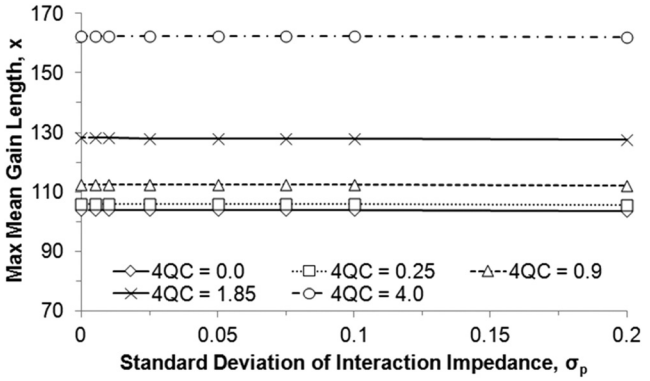


FIG. 12. Variation of length at which the maximum mean gain occurs with $C_0 = 0.019$ and $d = 0$ at different $4QC$ values as a function of the magnitude of random interaction impedance errors.

using $C_0 = 0.019$ and $d = 0$. Figure 11 shows the corresponding standard deviation. Figure 12 shows the corresponding axial TWT lengths at which the maximum mean backward-wave mode gain occurs. Figure 13 gives the calculated full-width instantaneous 1-dB bandwidth of the maximum mean gain in terms of $b$ for the same series of simulations.

### C. Random variation of the RF loss

Finally, we consider random variation of the Pierce loss parameter, $d$, along the length of a TWT. For this analysis, $d(x) = d_0 + d_1$ where $d_0$ is the unperturbed Pierce loss parameter and $d_1$ is a Gaussian random number defined by the standard deviation, $\sigma_d$. Since only positive values of $d$ represent RF loss in the simulation, it was necessary to set $d_0 = 0.5$ and limit $3\sigma_d < 0.5$.

Figures 14(a) and 14(b) show the absolute and relative variation of the maximum mean backward-wave mode gain as a function of the magnitude of Pierce loss parameter error at different $4QC$ values. These simulations were completed using $C = 0.019$ and $d_0 = 0.5$. Figure 15 shows the corresponding standard deviation. Figure 16 shows the corresponding axial TWT lengths at which the maximum mean backward-wave mode gain occurs. Figure 17 gives the calculated full-width instantaneous 1-dB bandwidth of the maximum mean gain with respect to $b$ for the same series of simulations.

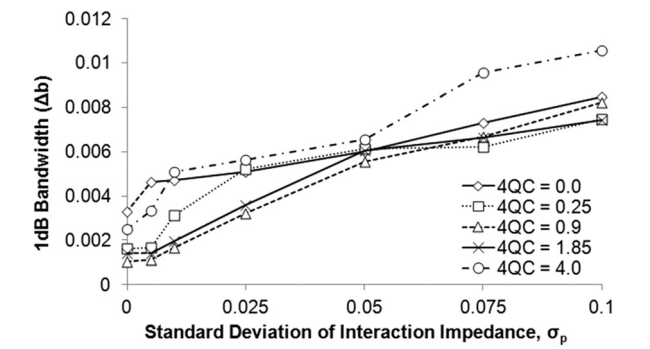


FIG. 13. Variation of 1-dB bandwidth of the maximum mean gain in terms of $b$ for $C_0 = 0.019$ and $d = 0$ at different $4QC$ values as a function of the magnitude of random interaction impedance errors.

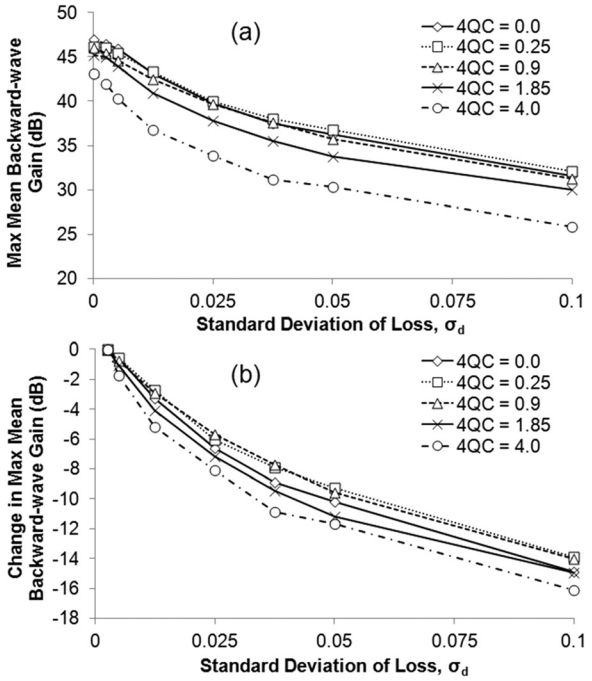


FIG. 14. Variation of maximum mean backward-wave mode gain for $C = 0.019$ and $d_0 = 0.5$ at different $4QC$ values as a function of the magnitude of random RF loss errors. The unnormalized results presented in (a) are normalized to the $\sigma_d = 0.0025$ case for each $4QC$ value in (b).

## IV. DISCUSSION

The data in Figs. 6, 10, and 14 show that the maximum mean backward-wave gain is significantly affected by all three types of errors tested. Phase velocity errors, however, have the largest relative impact. For example, from the data presented, a 10% phase velocity error (i.e., $\sigma_q = 0.1$) results in a backward-wave gain reduction of approximately 25 dB while a 10% interaction impedance error (i.e., $\sigma_p = 0.1$) or a 10% loss error (i.e., $\sigma_d = 0.1$) results in a gain reduction of only about 13 dB.

Surprisingly, from the same set of figures, it is observed that the magnitude of the space charge parameter, $4QC$, did not significantly affect the outcome of the backward-wave analysis. The only appreciable impact occurred during the random variation of RF loss as shown in Fig. 14. In that case, increasing $4QC$ lowered the overall maximum mean backward-wave gain.

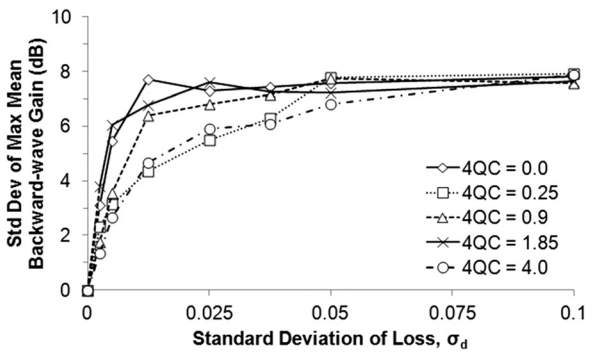


FIG. 15. Standard deviation of maximum mean backward-wave mode gain for $C = 0.019$ and $d_0 = 0.5$ at different $4QC$ values as a function of the magnitude of random RF loss errors.

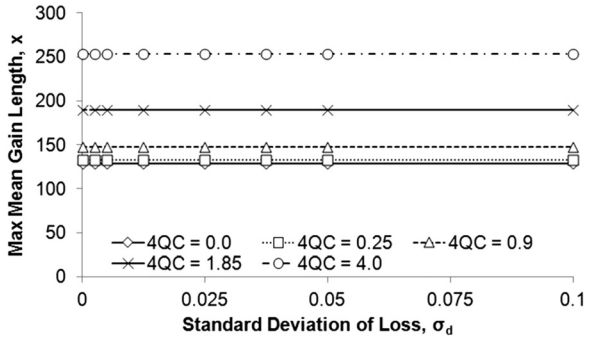


FIG. 16. Variation of length at which the maximum mean gain occurs with $C = 0.019$ and $d_0 = 0.5$ at different $4QC$ values as a function of the magnitude of random RF loss errors.

The limited impact of $4QC$ on the backward-wave gain can be explained by noting that the data presented in Figs. 6, 10, and 14 represent the *maximum* mean gain regardless of the axial length required to reach that gain. As shown in Figs. 8, 12, and 16, increasing the $4QC$ value results in an increased axial length at which the maximum mean gain occurs. By plotting the data this way, however, we can examine the worst-case, maximum backward-wave gain possible and how it is affected by the introduction of fabrication errors.

In Fig. 8, we observe that the introduction of phase velocity errors had an inconsistent effect on the maximum mean gain length (i.e., the axial length corresponding to the location where the maximum mean gain occurs). However, the effect was relatively modest and the results depended on the value of $4QC$ used in the simulation. Further study could be completed on this topic by reducing the numerical grid size in $x$ and repeating the analysis in order to better establish how the maximum mean gain length is affected by random phase velocity errors. Random variations of the interaction impedance and the loss had no discernible effect on the maximum mean gain length as shown in Figs. 12 and 16.

As shown in Figs. 7, 11, and 15, the standard deviation of the maximum mean gain for all three types of errors was similar in that all three start at zero for $\sigma = 0$ and approach approximately 7 dB as the standard deviation of the error type was increased. Subsequent inspection of the corresponding statistical distributions of the gain at various magnitudes of $\sigma$ verified these results. Further study is required

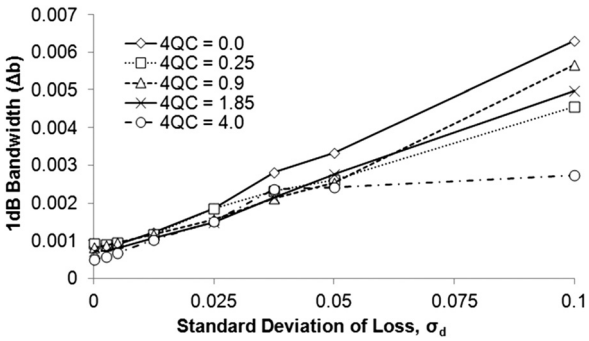


FIG. 17. Variation of 1-dB bandwidth of the maximum mean gain in terms of $b$ for $C = 0.019$ and $d_0 = 0.5$ at different $4QC$ values as a function of the magnitude of random RF loss errors.

to understand why the standard deviation of the gain behaves in this manner.

Finally, we observe from Figs. 9, 13, and 17 that the 1-dB bandwidth of the maximum mean backward-wave gain is approximately linearly related to the standard deviation of each type of error. When considered in combination with the results shown in Figs. 6, 10, and 14, we observe that regardless of the error type, increases in the error's standard deviation result in a decreased maximum mean gain value and increased 1-dB bandwidth. Of the three types of errors, phase velocity errors have the most significant impact on the bandwidth.

### A. Comparison of backward-wave and fundamental forward-wave mode results

It is of interest to compare the effect of fabrication errors on the maximum mean fundamental forward-wave and backward-wave mode gains while simultaneously looking at the impact on the fundamental forward-wave mode 1-dB bandwidth. We seek to explore whether random or quasi-random errors could be deliberately introduced into a SWS design in such a way that the backward-wave gain could be significantly reduced without significant reduction to either the fundamental forward-wave mode gain or bandwidth.

For this comparison, we used both the analysis derived here (for the backward-wave gain) and from previous work[8] (for the fundamental forward-wave gain and bandwidth). For consistency, the length of both the fundamental forward-wave and backward-wave models was set to the maximum mean gain length for the backward-wave for the particular set of Pierce parameters tested.

The value of the Pierce parameters was based on a previously developed 45 GHz ring-bar SWS design[15] whose basic design parameters are given in Table I. Namely, for the fundamental forward-wave mode $C = 0.028$ and for the backward-wave mode $C = 0.019$. The value of the fundamental forward-wave mode $C$ corresponds well with previously published mm-wave SWS design efforts.[16] In general, it is unlikely that the value of $C$ will be identical for the fundamental forward-wave and backward-wave modes since the interaction impedances will likely differ. Although it is difficult to generalize these results to all possible TWT designs, it is generally the case for well-designed TWTs that the backward-wave interaction impedance is significantly less than the fundamental forward-wave mode.

The $4QC$ parameter was set to 0.9 and 1.85 for the fundamental forward-wave and backward-wave modes, respectively. Again, these values were based on the ring-bar SWS design and correspond well with previously published design values.[16]

The TWT was assumed lossless (i.e., $d = 0$ for both modes) except when $d$ was allowed to randomly vary along the length of the SWS. As discussed earlier, in that case, $d_0$, was set to 0.5 to ensure that $d$ remained a positive value.

The comparison of the maximum mean fundamental forward-wave and backward-wave mode gains and the impact on the fundamental forward-wave mode's maximum mean gain 1-dB bandwidth are shown in Fig. 18. In each case, it is observed that the backward-wave mode gain drops much more rapidly than does the forward-wave gain as random error is introduced. This is in part because the maximum mean backward-wave gain is ideally infinite in the error-free case. In other words, when errors are not present, the TWT is susceptible to an absolute instability for interaction lengths greater than that required for start oscillation. As

TABLE I. Design parameters for the 45 GHz ring-bar SWS.

| | |
|---|---|
| Beam voltage (V) | 14 350 |
| Beam current density (A/cm$^2$) | 62.5 |
| Gain per stage (dB) | ~20-30 |
| RF efficiency (%) | ~10 |
| Center frequency | 45 GHz |

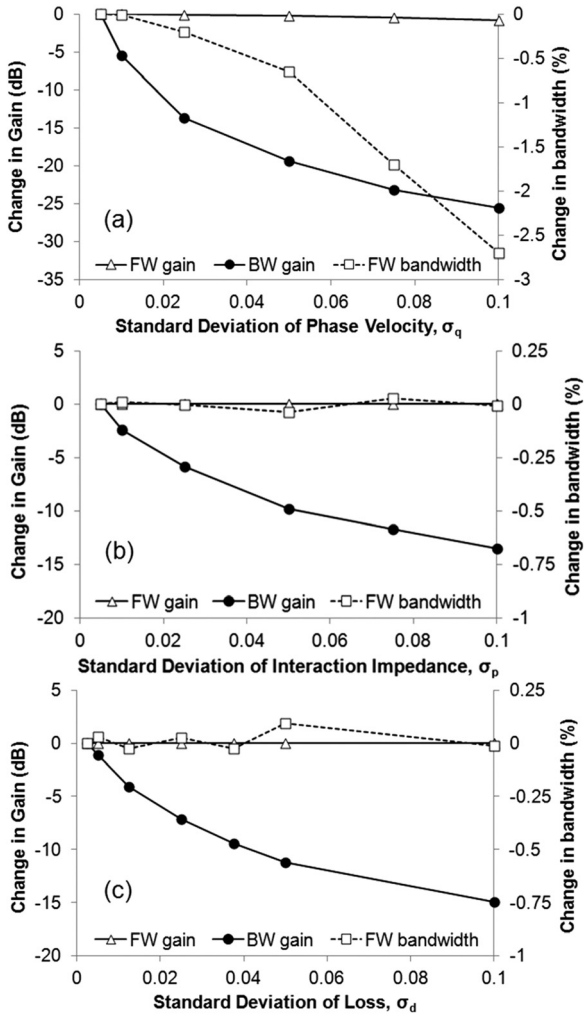


FIG. 18. Comparison of maximum mean fundamental forward- and backward-wave mode gains and change in fundamental forward-wave 1-dB bandwidth of the maximum mean gain with introduction of random errors along the length of a simulated TWT. Phase velocity errors were introduced in (a), interaction impedance errors in (b), and loss errors in (c). The mean values for the Pierce parameters were set based on the ring-bar SWS design in which $(C_0)_{fund.} = 0.028$, $(C_0)_{back.} = 0.019$, $4QC_{fund.} = 0.9$, and $4QC_{back.} = 1.85$. The mean value of loss was set to $d_{fund.} = d_{back.} = 0$ for (a) and (b) and set to $(d_0)_{fund.} = (d_0)_{back.} = 0.5$ for (c). The data were normalized to the results for $\sigma_q = 0.005$ for (a), $\sigma_p = 0.005$ for (b), and $\sigma_d = 0.0025$ for (c).

errors are added, this absolute instability is lost and the maximum mean gain of the backward-wave mode drops rapidly from infinity.

The largest decrease of the backward wave gain occurred when random phase velocity errors were introduced. In this example, a 5% random phase velocity error reduced the maximum backward-wave gain by approximately 19 dB while only decreasing the fundamental forward-wave mode gain by 0.6 dB and reducing the fundamental forward-wave's maximum mean gain 1-dB bandwidth by 0.7%. This is a significant result since it is reasonable that a 5% phase velocity variation could be realized in a SWS design. If one deliberately designed a 5% phase velocity variation into a nominal SWS in a TWT, the gain of the backward-wave mode could be reduced without significant impact on the fundamental forward-wave mode gain or bandwidth. This ultimately would produce a TWT that is more stable against unwanted oscillations without significantly affecting fundamental forward-wave mode performance.

For the example displayed in Table I, the phase velocity error is of order 1%; detailed dimensional measurements and statistical analysis on this TWT have been previously presented.[15] Note that with $\sigma_q = 0.01$ and $C = 0.028$ (i.e., the nominal value used for the fundamental forward-wave mode in this paper), then $\sigma_b = \sigma_q/C = 0.01/0.028 = 0.357$, which is within the range displayed in Fig. 8 of Chernin *et al.*[9]

It should be reiterated that the current model does not include the effects of multiple internal RF reflections from the discontinuities. When internal reflections are included, Chernin *et al*. have previously demonstrated that random variation of a SWS pitch can have significant impact on TWT performance by introducing small-signal gain ripple.[9] Therefore, it is likely that a TWT designer that deliberately introduces phase velocity errors would be faced with a trade-off between backward-wave oscillation suppression and the magnitude of small-signal gain ripple. Analyzing this trade-off is of interest for future study.

We also see from Figs. 18(b) and 18(c) that random interaction impedance and loss errors can also impact TWT performance. In this example, a 5% random interaction impedance error resulted in a reduction of the backward-wave gain of approximately 10 dB while a 5% random loss error resulted in a backward-wave gain reduction of approximately 12 dB. Neither had appreciable effects on the fundamental forward-wave mean gain or 1-dB bandwidth.

From these results, we conclude that random or quasi-random variations of the circuit parameters (i.e., phase velocity, interaction impedance, and/or loss) along the length of the TWT have the potential to significantly reduce unwanted backward-wave gain while only having a minor effect on fundamental forward-wave mode performance. Although beyond the scope of the present work, it would be of interest to explore how to best utilize these results in a TWT and investigate how to best realize deliberate circuit parameter variations in the fabrication of a SWS.

## V. CONCLUSION

We have developed a model to look at the impact of random fabrication errors (encoded as random variations of the Pierce parameters along the length of a simulated TWT) on the backward-wave mode. Phase velocity errors were shown to reduce the backward-wave gain most significantly although both interaction impedance and loss errors also had significant impacts. The magnitude of the space charge forces, $4QC$, did not appear to have a substantial impact on the calculated maximum mean backward-wave gain but did affect the axial length at which the maximum gain occurs (i.e., the oscillation length). For example, increasing the $4QC$ value resulted in a longer start oscillation length. The 1-dB bandwidth (with respect to $b$) of the backward-wave mode's maximum mean gain was found to be linearly related to the standard deviation of the Pierce parameter errors and, again, phase velocity errors had the largest effect.

In comparing the effect of random fabrication errors on the fundamental forward-wave and backward-wave mode gains and bandwidths, we identified that a 5% random variation of the circuit parameters (i.e., phase velocity, interaction impedance, or loss) along the length of a SWS can significantly reduce backward-wave gain while having only a minor effect on fundamental forward-wave mode gain and bandwidth. This is a significant result that could be utilized to produce TWTs that are more stable against unwanted oscillations while having essentially the same fundamental forward-wave mode performance.

## ACKNOWLEDGMENTS

This work was supported by L-3 Communications – Electron Devices Division, San Carlos, CA 95070.

[1]J. H. Booske, Phys. Plasmas **15**, 055502-1 (2008).
[2]J. H. Booske, R. J. Dobbs, C. D. Joye, C. L. Kory, G. R. Neil, G.-S. Park, J. Park, and R. J. Temkin, IEEE Trans. Terahertz Sci. Technol. **1**, 54 (2011).
[3]S. Sensiper, Proc. IRE **43**, 149 (1955).
[4]J. R. Pierce, *Traveling Wave Tubes* (D. Van Nostrand, Princeton, NJ, 1950).
[5]R. G. Hutter, *Beam and Wave Electronics in Microwave Tubes* (D. Van Nostrand, Princeton, NJ, 1960).
[6]J. E. Rowe, *Nonlinear Electron-Wave Interaction Phenomenon* (Academic, New York, NY, 1965).
[7]P. Pengvanich, D. Chernin, Y. Y. Lau, J. W. Luginsland, and R. M. Gilgenbach, IEEE Trans. Electron Devices **55**, 916 (2008).
[8]S. Sengele, M. Barsanti, T. A. Hargreaves, C. M. Armstrong, J. H. Booske, and Y. Y. Lau, IEEE Trans. Electron Devices (to be published).
[9]D. Chernin, I. Rittersdorf, Y. Y. Lau, T. M. Antonsen, Jr., and B. Levush, IEEE Trans. Electron Devices **59**, 1542 (2012).
[10]Y. Y. Lau and D. Chernin, Phys. Fluids B **4**, 3473 (1992).
[11]H. R. Johnson, Proc. IRE **43**, 684 (1955).
[12]S. Ramo, Proc. IRE **27**, 584 (1939).
[13]A. S. Gilmour, *Principles of Traveling Wave Tubes* (Artech House, Norwood, MA, 1994).
[14]T. M. Antonsen, Jr., P. Safier, D. P. Chernin, and B. Levush, IEEE Trans. Plasma Sci. **30**, 1089 (2002).
[15]S. Sengele, Ph.D. dissertation, University of Wisconsin – Madison, 2012.
[16]J. H. Booske, M. C. Converse, C. L. Kory, C. T. Chevalier, D. A. Gallagher, K. E. Kreischer, V. O. Heinen, and S. Bhattacharjee, IEEE Trans. Electron Devices **52**, 685 (2005).